Available online at www.sciencedirect.com
ScienceDirect
Bioorganic & Medicinal Chemistry Letters 18 (2008) 726–731
Bioorganic & Medicinal Chemistry Letters

Optimization of biaryl Selective HDAC1&2 Inhibitors (SHI-1:2)

David J. Witter,[a,*] Paul Harrington,[a,†] Kevin J. Wilson,[a] Melissa Chenard,[c] Judith C. Fleming,[b] Brian Haines,[c] Astrid M. Kral,[b] J. Paul Secrist[b] and Thomas A. Miller[a]

[a]*Department of Drug Design and Optimization—Medicinal Chemistry, Merck Research Laboratories, 33 Avenue Louis Pasteur, Boston, MA 02115, USA*
[b]*Department of Cancer Biology and Therapeutics, Merck Research Laboratories, 33 Avenue Louis Pasteur, Boston, MA 02115, USA*
[c]*Department of Pharmacology, Merck Research Laboratories, 33 Avenue Louis Pasteur, Boston, MA 02115, USA*

Received 18 October 2007; revised 12 November 2007; accepted 14 November 2007
Available online 19 November 2007

Abstract—A class of biaryl benzamides was identified and optimized as selective HDAC1&2 inhibitors (SHI-1:2). These agents exhibit selectivity over class II HDACs 4–7, as well as class I HDACs 3 and 8; providing examples of selective HDAC inhibitors for the HDAC isoforms most closely associated with cancer. The hypothesis for the increased selectivity is the binding of a pendant aromatic group in the internal cavity of the HDAC1&2 enzymes. SAR development based on an initial lead led to a series of potent and selective inhibitors with reduced off-target activity and tumor growth inhibition activity in a HCT-116 xenograft model.

HDAC1 and HDAC2 are class I histone deacetylase (HDAC) enzymes and are members of a broader family of 11 zinc-dependent HDAC enzymes, which are emerging therapeutic targets for the treatment of cancer and other diseases.[1] These enzymes, as part of multi-protein complexes, catalyze the removal of acetyl groups from lysine residues on proteins, including histones, affecting gene expression, differentiation, growth arrest, and/or apoptosis in transformed cell cultures.[2]

While the biological functions of the various HDAC subtypes are only partially understood, HDAC1 and HDAC2 have documented roles in regulating cell proliferation and represent compelling targets for cancer therapeutics.[3,4] RNAi-mediated knockdown of HDAC1 expression inhibits proliferation and, importantly, induces apoptosis in several tumor cell lines in vitro.[3] Mutations and inactivations of histone acetyltransferases (HATs) and overexpression of HDAC1 and HDAC2 have been observed in certain cancers.[4] The mounting evidence for the involvement of HDAC1 and HDAC2 in cancer suggests that inhibitors selective for these subtypes may demonstrate an improved therapeutic index through enhanced clinical efficacy and/or better tolerability compared to pan HDAC inhibitors. Since all current clinical HDAC inhibitors appear to inhibit HDAC1, HDAC2, and HDAC3, as well as other HDAC subtypes,[5] our program sought to identify selective inhibitors that target HDAC1 and HDAC2 preferentially.[6]

A wide range of structures have been shown to inhibit the activity of class I/II HDAC enzymes and, with few exceptions, these can be broadly characterized by a common pharmacophore[7] comprised of a metal binding domain, a linker domain, and a surface-recognition domain, exemplified by Zolinza® (SAHA, vorinostat), which was recently approved for the treatment of cutaneous manifestations of cutaneous T-cell lymphoma (Fig. 1).[8] Initial SHI-1:2 design considerations included minimizing strong metal binding moieties (e.g., hydroxamic acids) to decrease the potential for general metal binding related 'promiscuity' and leveraging available structural data to guide the development of compounds with enhanced potency and selectivity. For example, the presence of an extensive internal cavity near the active site of HDAC family members suggests

Keywords: Histone deacetylase; HDAC; Aminobenzamides; Biaryl.
* Corresponding author. Tel.: +1 617 992 2067; fax: +1 617 992 2403; e-mail: David_Witter@Merck.com
† Present address: Department of Medicinal Chemistry, Amgen Inc., One Amgen Center Drive, Thousand Oaks, CA 91320-1799, USA.

0960-894X/$ - see front matter © 2007 Elsevier Ltd. All rights reserved.
doi:10.1016/j.bmcl.2007.11.047

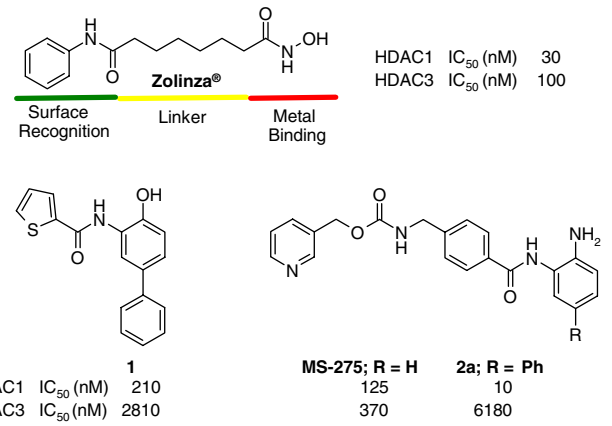

Figure 1. Zolinza®, Biaryl **1**, MS-275, and SHI-1:2 **2a**.

that modification of the zinc-binding domain could provide a rational approach to selective inhibitor design.[9] The size and composition of the cavity predicted in HDAC1 suggests that a large hydrophobic group can be accommodated in the interior of the enzyme active site. Gratifyingly, biaryl-phenol **1**, which was discovered as a hit during an HTS campaign, was found to be a potent inhibitor of HDAC1 enzyme preparations and is 10-fold less potent against HDAC3 (Fig. 1 and Table 1). Since biaryl-phenol **1** lacks an extensive linker domain and does not possess a surface-recognition domain, it represents a novel starting point for SAR generation. Further, the structural similarity between **1** and the existing class of benzamide HDAC inhibitors, typified by MS-275 (Fig. 1), suggested that modification of the linker domain and addition of a more extensive surface-recognition domain was feasible. To assess the proposed binding mode for the biaryl HDAC1 selective inhibitors, the biaryl structural analog of the clinical agent MS-275 was prepared (**2a**, Fig. 1). Compound **2a** was found to be a potent and selective HDAC1 inhibitor, whereas MS-275 is only 3-fold selective for HDAC1 (125 nM) over HDAC3 (370 nM). In light of these findings, we undertook an extensive SAR program to further enhance and characterize the activities of the biaryl class of selective HDAC1&2 inhibitors (SHI-1:2; Selective HDAC1&2 Inhibitor(s)).

The synthesis of SHI-1:2 **2a** is shown in Scheme 1. Commercially available 4-bromo-2-nitroaniline (**3**) was Boc-protected and arylated with phenyl boronic acid using Suzuki cross-coupling. The resultant nitro-biaryl **4** was hydrogenated to the mono Boc-protected dianiline **5**. The acid **8** was generated from CDI coupling of 3-pyridinemethanol (**6**) and 4-(aminomethyl)benzoic acid (**7**). Coupling conditions with BOP led to the Boc-protected **9a**, which was deprotected with TFA to generate the desired amino-biaryl **2a**.[10]

Table 1. HDAC selectivity of Zolinza®, **1**, MS-275, and SHI-1:2 **2a**

HDAC	IC_{50}[a] (nM)			
	Zolinza™	**1**	MS-275	**2a**
1	30	210	125	10
2	170	ND	340	72
3	100	2810	370	6180
4	>50,000	ND	>50,000	>50,000
5	>30,000	ND	>50,000	>50,000
6	38	>50,000	>50,000	>50,000
7	>30,000	ND	>50,000	>30,000
8	410	ND	14,120	>20,000

[a] Values are means of three experiments. ND = not determined.

The extent of subtype selectivity of SHI-1:2 **2a** across HDAC class I and II family members was measured in vitro by monitoring the deacetylation of a synthetic acetyl-lysine bearing peptide by subtype-specific HDAC complexes purified from mammalian cells overexpressing recombinant enzyme.[11] Zolinza®, which is generally considered a broad spectrum inhibitor, is selective for the class I and limited class II HDAC enzymes (1–3, 6, 8) with IC_{50} values ranging from 40 to 410 nM for these family members, but possesses IC_{50} values >30,000 nM for the class II enzymes (4, 5, and 7). MS-275 shares a similar profile to Zolinza®, with the exception of HDAC6 and HDAC8 inhibition where greater than 110- and 400-fold selectivities are observed, respectively. Biaryl lead **1** exhibits HDAC1 potency similar to MS-275, but possesses greater than 10-fold selectivity over HDAC3. SHI-1:2 **2a** is selective over all HDAC isoforms tested. The lowest selectivity observed relative to HDAC1 is 7-fold over HDAC2.

Having demonstrated that the biaryl structural class of SHI-1:2 possesses a high degree of HDAC selectivity, we wanted to explore additional analogs and test the anti-proliferative activities of these agents in a cell-based assay.[12]

Additional SHI-1:2 **2a** analogs were prepared via the synthetic pathway depicted in Scheme 2. Amide formation with chloromethyl benzoyl chloride and the Boc-protected biaryl benzamide generates the chloromethyl intermediate **11a**, which is converted to free amine **12a** via phthalimide displacement of the chloride and subsequent deprotection. Acylation of the resulting amine generates the desired amide or carbamate analogs **14a–i** after TFA deprotection.[10]

We initially explored subtle changes to the carbamate core of **2a** to determine the effects on HDAC1 and cell-based activity (Table 2). Analog **14a**, which is the corresponding amide of carbamate **2a**, exhibited similar enzymatic and cellular activity to the parent **2a**. However, replacement of the 3-pyridyl with 2-pyridyl (**14b**) or phenyl (**14c**) resulted in reduced anti-proliferative potency. Moreover, removal of the methylene spacer in **2a**, generating phenyl carbamate **14d**, also decreased activity in the HCT-116 assay.

The ancillary pharmacology profiles of the SHI-1:2 carbamate analogs were also gathered to investigate off-target activities (Table 2). CYP inhibition potential was determined against a number of human isoforms, and ion channel affinity in a displacement binding assay using radio-labeled MK-499.[13] SHI-1:2 **2a** was found to be an inhibitor of CYP isoforms and it

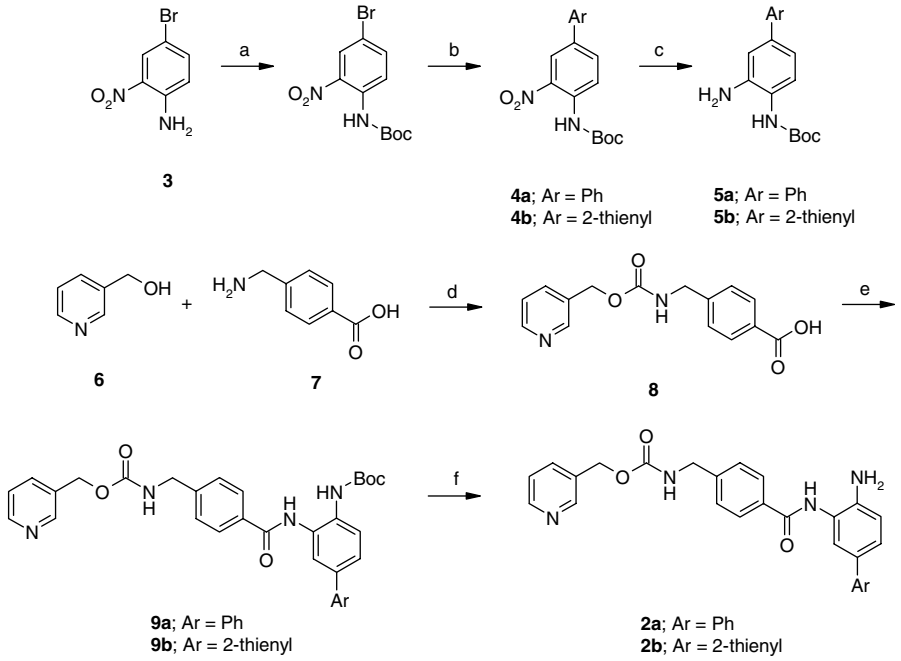

Scheme 1. Reagents: (a) Boc_2O, Et_3N, DCM (62%); (b) Ar-$B(OH)_2$, K_2CO_3, $Pd(PPh_3)_4$, THF (89–95%); (c) H_2, Pd/C, MeOH (72–80%); (d) CDI, DBU, THF (80%); (e) **5a** or **5b**, EDCI, HOBt, DMF (75–85%); (f) TFA, DCM (60–70%).

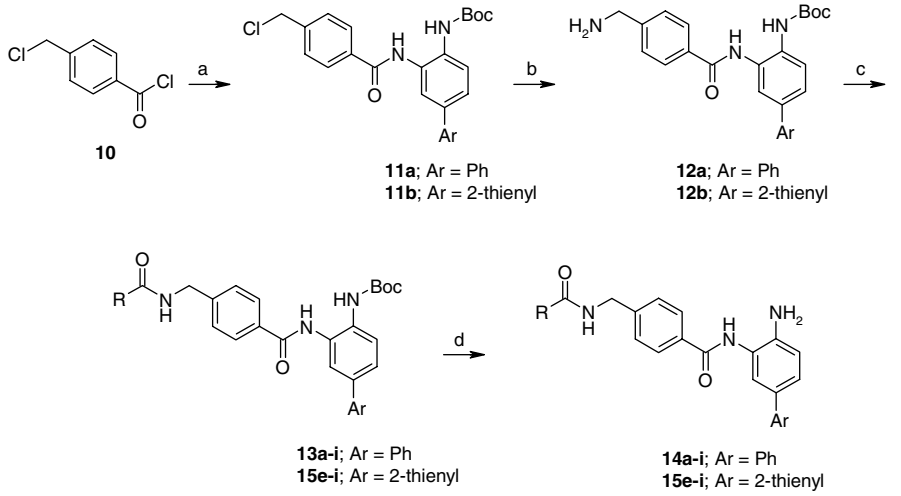

Scheme 2. Reagents: (a) **5a** or **5b**, *i*-$PrEt_2N$, THF (90–94%); (b) phthalimide, K_2CO_3, KI, Tol (68–75%); (ii) NH_2NH_2, EtOH (67–77%); (c) RC(O)Cl, *i*-$PrEt_2N$, THF or ROH, CDI, THF or ROC(O)Cl, *i*-$PrEt_2N$, THF or RCO_2H, HATU; (d) TFA, DCM.

exhibits IKr ion channel binding activity (IC_{50} 3.0 μM). The CYP inhibition for **2a** was greatest for CYP3A4 with 70% at 1 μM. Both CYP2D6 and CYP2C9 were also affected but to a lesser extent, 69% and 71% at 10 μM, respectively. The 3-pyridyl amide **14a** faired better than the parent with respect to both IKr binding as well as CYP inhibition. For 2-pyridyl analog **14a**, the IKr binding and CYP3A4 inhibition were also attenuated. The benzyl and phenyl analogs, **14c** and **14d**, respectively, did not appreciably inhibit CYP enzymes or display IKr binding. Based on these results, additional analogs were explored to maintain the clean off-target activity, but improve biochemical and anti-proliferation activities of the initial carbamate analogs.

Based on the off-target activity issues noted with the 3-pyridylmethyl carbamate, additional analogs were explored focusing on alkyl substituents. Accordingly, the ethyl and methyl carbamate analogs of **2a** were prepared, affording **14e** and **14f**, respectively, which maintain potent enzymatic and cellular activity (Table 3). Gratifyingly, CYP inhibition and IKr ion channel binding activities were greatly attenuated. The desired trend of reduced off-target activity continued with amide analogs **14g** and **14h**. The HDAC1 enzymatic inhibitory activities for **14g** and **14h** were $IC_{50} = 10$ nM for both analogs and the anti-proliferation activities were $GI_{50} = 220$ and 150 nM, respectively, indicating tolerance for various moieties in the recognition domain. Larger alkyl groups are acceptable in the recognition

Table 2. The initial series of biaryl SHI-1:2

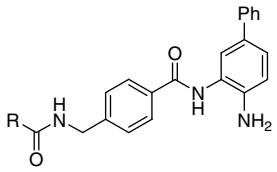

	R	HDAC1 IC_{50}[a] (nM)	HCT-116 GI_{50}[a] (nM)	% MK-499 Binding Inhibition at 10 μM	% CYP Inhibition at 10 μM 3A4	2C9	2D6
2a	3-Pyridyl-CH_2O	10	225	IC_{50} = 3.0 μM	70 at 1 μM	69	71
14a	3-Pyridyl-$(CH_2)_2$	11	337	IC_{50} = 3.7 μM	65	73	25
14b	2-Pyridyl-CH_2O	8	435	51	38	67	29
14c	BnO	17	820	30	28	27	16
14d	PhO	16	1440	15	22	21	12

[a] Values are means of $n \geqslant 2$ experiments.

Table 3. The alkyl carbamate and amide series of biaryl SHI-1:2

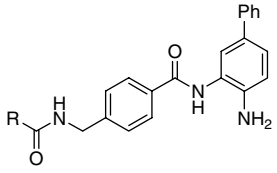

	R	HDAC1 IC_{50}[a] (nM)	HCT-116 GI_{50}[a] (nM)	% MK-499 Binding Inhibition at 10 μM	% CYP Inhibition at 10 μM 3A4	2C9	2D6
2a	3-Pyridyl-CH_2O	10	225	IC_{50} = 3.0 μM	70 at 1 μM	69	71
14e	EtO	13	230	40	22	35	26
14f	MeO	10	230	28	23	46	49
14g	*n*-Pr	10	220	38	33	27	28
14h	Et	10	150	24	30	28	38
14i	Cyclohexyl-	20	335	30	12	32	17

[a] Values are means of $n \geqslant 2$ experiments.

domain. Cyclohexyl amide **14i**, for example, has slightly reduced enzyme and anti-proliferative activities with minimal off-target activity.

To further investigate the SAR of the pendant phenyl group of the biaryl SHI-1:2, a series of 2-thienyl substituted analogs (**15e–i**) was prepared. These agents, which were prepared in a manner analogous to that used for the phenyl analogs (Schemes 1 and 2), demonstrated similar, although slightly greater, activity relative to the phenyl derivatives **14e–i** (Table 4).

To verify that HDAC1&2 selectivity was maintained during the lead optimization process, representative examples were tested against a panel of HDAC isoforms (Table 5). The HDAC selectivity data reveal that the biaryl benzamide moiety confers selectivity for HDAC1 and HDAC2 over the other HDACs tested.[14] The HDAC activity was greatly attenuated for not only the class II HDACs 4–7, but also the other members of class I HDACs, 3 and 8. Moreover, there was a slight preference for HDAC1 over HDAC2.

Based on the desirable off-target profile of methyl carbamate **14f**, the pharmacologic properties of this analog were tested in vivo for the ability to attenuate tumor growth in an HCT-116 colon xenograft model in nude mice (Fig. 2). The methyl carbamate demonstrated marked dose dependent efficacy (50, 100, and 150 mg/kg po qd) at tolerated doses (<10% body weight loss)

Table 4. The 2-thienyl series of biaryl SHI-1:2

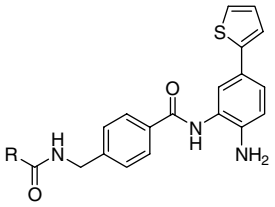

	R	HDAC1 IC_{50}[a] (nM)	HCT-116 GI_{50}[a] (nM)
2b	3-Pyridyl-CH_2O	6	155
15e	EtO	7	130
15f	MeO	6	100
15g	*n*-Pr	9	135
15h	Et	9	146
15i	Cyclohexyl-	13	185

[a] Values are means of $n \geqslant 2$ experiments.

Table 5. HDAC selectivity of SHI-1:2 analogs, **2b**, **14f**, **15e**, and **15f**

HDAC	IC_{50}[a] (nM)			
	2b	**14f**	**15e**	**15f**
1	6	13	7	10
2	190	115	71	105
3	27,710	22,450	>50,000	>50,000
4	>50,000	>50,000	>50,000	>50,000
5	ND	>50,000	>50,000	ND
6	>50,000	>50,000	>50,000	>50,000
7	ND	>50,000	>50,000	ND
8	31,738	>50,000	>50,000	>50,000

[a] Values are means of three experiments. ND = not determined.

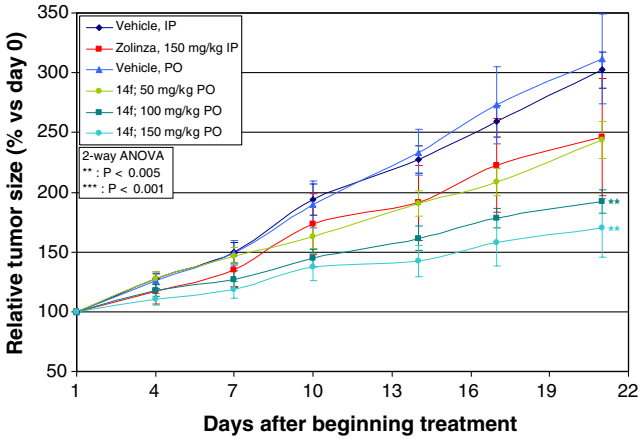

Figure 2. HCT-116 mouse xenograft model with Zolinza® and **14f**.

when orally dosed once daily for 21 days. The tumor growth inhibition at 50 mg/kg qd was equivalent to Zolinza® (150 mg/kg ip qd).

The structural details of HDAC inhibitor/enzyme interactions were first elucidated by Finnin et al. in 1999.[9] The crystal structure of histone deacetylase-like protein (HDLP), a homolog of mammalian HDAC1 with ~35% sequence identity, was solved with Zolinza® bound to the active site. The structural findings revealed that HDLP has a tubelike 11 Å deep channel wherein the alkyl chain of Zolinza® resides and the hydroxamate chelates with the catalytic zinc (Fig. 3A). Immediately adjacent to the active site zinc is 14 Å long internal cavity lined primarily with hydrophobic residues. The internal cavity's function is postulated to be a diffusion pathway for the acetate by-product after enzymatic hydrolysis.[15] We hypothesize that the novel class of biaryl SHI-1:2 bind to this internal cavity via the pendant aryl moiety of the biaryl benzamide headgroup (Fig. 3B) and that differences in the various HDAC family member's active sites and internal cavities lead to a preference for the biaryl headgroup with the HDAC1 isoform. The crystal structure of the hHDAC8 supports this hypothesis, since the presence of the Trp-141 at the bottom of the active site channel could block the zinc chelation with the aminobenzamide.[16] Moreover, the shape of the internal cavity of hHDAC8 differs from that proposed for HDAC1. Based on the utilization of

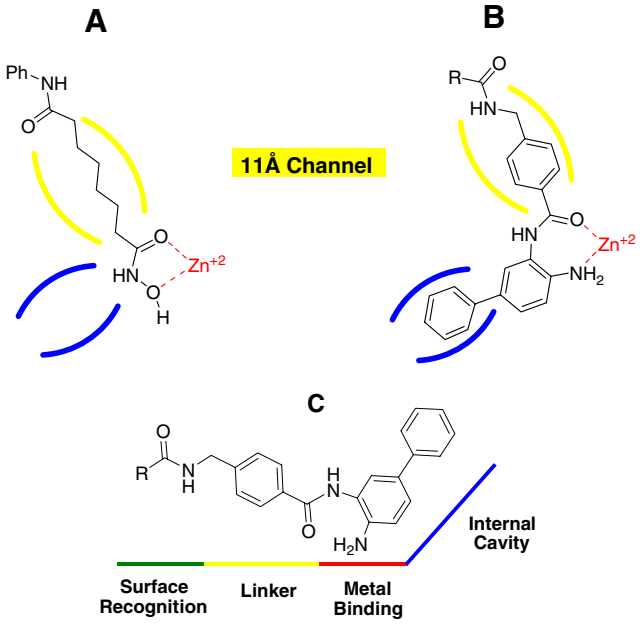

Figure 3. Schematic representation of Zolinza® and a biaryl SHI-1:2 analog bound in the HDAC1 active site. (A) Zolinza® bound in HDLP occupying the hydrophobic channel depicted in yellow. (B) Biaryl SHI-1:2 occupying both the channel (yellow) and internal cavity depicted in blue. (C) New pharmacophore model for selective HDAC inhibition (SHI-1:2).

the HDAC1 internal cavity, we propose refinement of the current HDAC pharmacophore model to include the internal cavity as depicted in Figure 3. In-house docking studies using a homology model of hHDAC1[17] support this hypothesis.

In conclusion, we have identified a series of biaryl benzamides that are selective HDAC1&2 inhibitors (SHI-1:2), exhibiting selectivity over class II HDACs 4–7, as well as class I HDACs 3 and 8. The biaryl class of SHI-1:2 analogs provide an example of selective HDAC inhibitors for the HDAC isoforms most closely associated with cancer. The hypothesis for the increased HDAC selectivity is the binding of the pendant aromatic group in the internal cavity of the HDAC isoform. SAR development based on initial lead **1** led to a series of potent and selective inhibitors with in-vivo xenograft activity and acceptable off-target activity. The therapeutic advantages that greater selectivity offers with regard to an improved tolerability and efficacy compared to Zolinza® and other less selective HDAC inhibitors require further preclinical and clinical examination. Additional studies of SHI-1:2 **2a** and related analogs will be reported in due course.

References and notes

1. (a) Huang, L. *J. Cell. Physiol.* **2006**, *209*, 611; (b) Liu, T.; Kuljaca, S.; Tee, A.; Marshall, G. M. *Cancer Treatment Rev.* **2006**, *32*, 157; (c) Sadri-Vakili, G.; Cha, J.-H. J. *Curr. Alzh. Res.* **2006**, *3*, 403.
2. (a) Rodriquez, M.; Aquino, M.; Bruno, I.; De Martino, G.; Taddei, M.; Gomez-Paloma, L. *Curr. Med. Chem.*

2006, *13*, 1119; (b) Dokmanovic, M.; Marks, P. A. *J. Cell. Biochem.* **2005**, *96*, 293.
3. Glaser, K. B.; Li, J.; Staver, M. J.; Wei, R.-Q.; Albert, D. A.; Davidsen, S. K. *Biochem. Biophys. Res. Commun.* **2003**, *310*, 529.
4. (a) Kishimoto, M.; Kohno, T.; Okudela, K.; Otsuka, A.; Saski, H.; Tanabe, C.; Sakiyama, T.; Hirama, C.; Kitabayashi, I.; Minna, J. D.; Takenoshita, S.; Yokota, J. *Clin. Cancer Res.* **2005**, *11*, 512; (b) Ishihama, K.; Yamakawa, M.; Semba, S.; Takeda, H.; Kawata, S.; Kimura, S.; Kimura, W. *J. Clin. Pathol.* **2007**, *24*, 1; (c) Zhu, P.; Martin, E.; Mengwasser, J.; Schlag, P.; Janssen, K.-P.; Göttlicher, M. *Cancer Cell* **2004**, *5*, 455; (d) Senese, S.; Zaragoza, K.; Minardi, S.; Muradore, I.; Ronzoni, S.; Passafaro, A.; Bernard, L.; Draetta, G. F.; Alcalay, M.; Seiser, C.; Chiocca, S. *Mol. Cell. Biol.* **2007**, *27*, 4784; (e) Ropero, S.; Fraga, M. F.; Ballestar, E.; Hamelin, R.; Yamamoto, H.; Boix-Chornet, M.; Caballero, R.; Alaminos, M.; Setien, F.; Paz, M. F.; Herranz, M.; Palacios, J.; Arango, D.; Orntoft, T. F.; Aaltonen, L. A.; Schwartz, S., Jr.; Esteller, M. *Nat. Genet.* **2006**, *38*, 566.
5. Glaser, K. B. *Biochem. Pharm.* **2007**, *74*, 659.
6. During this manuscript submission, a reference was released via JMC web-site. Moradei, O. M.; Mallais, T. C.; Frechette, S.; Paquin, I.; Tessier, P. E.; Leit, S. M.; Fournal, M.; Bonfils, C.; Trachy-Bourget, M.-C.; Liu, J.; Yan, T. P.; Lu, A.-H.; Rahil, J.; Wang, J.; Lefebvre, S.; Li, Z.; Vaisburg, A. F.; Besterman, J. M. *J. Med. Chem.* **2007**, ASAP.
7. Miller, T. A.; Witter, D. J.; Belvedere, S. *J. Med. Chem.* **2003**, *46*, 5097.
8. Grant, S.; Easley, C.; Kirkpatrick, P. *Nature Rev. Drug Discov.* **2007**, *6*, 21.
9. Finnin, M. S.; Donigian, J. R.; Cohen, A.; Richon, V. M.; Rifkind, R. A.; Marks, P. A.; Breslow, R.; Pavletich, N. P. *Nature* **1999**, *401*, 188.
10. Spectral data for **2a/14f**: **2a**; ^{1}H NMR (d_6-DMSO, 600 MHz) δ 9.69 (s, 1H), 8.57 (s, 1H), 8.51 (dd, J = 4.8 and 1.8 Hz, 1H), 7.94 (m, 3H), 7.77 (d, J = 7.8 Hz, 1H), 7.53 (d, J = 7.8 Hz, 2H), 7.50 (d, J = 1.8 Hz, 1H), 7.37 (m, 5H), 7.31 (dd, J = 8.4 and 1.8 Hz, 1H), 7.22 (t, J = 7.8 Hz, 1H), 6.84 (d, J = 8.4 Hz, 1H), 5.08 (br s, 4H), 4.26 (d, J = 6.0 Hz, 2H); MS: Calcd 453 (MH^+), exp 453 (MH^+). **14f;**^{1}H NMR (d_6-DMSO, 600 MHz) d 9.86 (s, 1H), 8.73 (s, 1H), 7.90 (d, J = 8.4 Hz, 2H), 7.81 (d, J = 1.8 Hz, 1H), 7.75 (t, J = 6.0 Hz, 1H), 7.61 (m, 3H), 7.48 (dd, J = 9.0 and 3.6 Hz, 1H), 7.43 (t, J = 8.1 Hz, 2H), 7.38 (d, J = 8.4 Hz, 2H), 7.32 (t, J = 7.5 Hz, 1H), 4.23 (d, J = 6.0 Hz, 2H), 3.53 (s, 3H), 1.42 (s, 9H); MS: Calcd 376 (MH^+), exp 376 (MH^+).
11. See reference within Jones, P.; Altamura, S.; Chakravarty, P. K.; Cecchetti, O.; De Francesco, R.; Gallinari, P.; Ingenito, R.; Meinke, P. T.; Petrocchi, A.; Rowley, M.; Scarpelli, R.; Serafini, S.; Steinkühler, C. *Bioorg. Med. Chem. Lett.* **2007**, *16*, 5948.
12. HDAC cell-based proliferation results were determined by the following procedure: HCT116 cells were plated in 96-well plates at a density of 1000 cells/well. The next day, cells were treated with either 0.2% DMSO or increasing concentrations of **7i** dissolved in DMSO (final concentration DMSO 0.2%). After 72 h incubation at 37 °C with 5% CO_2, viable cells were quantitated using Vialight Plus (Cambrex) according to manufacturer's instructions.
13. Wang, J.; Della Penna, K.; Wang, H.; Karczewski, J.; Connolly, T. M.; Koblan, K. S.; Bennett, P. B.; Salata, J. J. *Am. J. Physiol.* **2003**, *284*, H256.
14. HDAC3 IC_{50} biochemical data for all compounds in the manuscript are at least >10 μM, where the value is not shown within.
15. Wang, D.-F.; Wiest, O.; Helquist, P.; Lan-Hargest, H. Y.; Wiesch, N. L. *J. Med. Chem.* **2004**, *47*, 3409.
16. Vannini, A.; Volpari, C.; Filocamo, G.; Casavola, E. C.; Brunetti, M.; Renzoni, D.; Chakravarty, P.; Paolini, C.; De Francesco, R.; Gallinari, P.; Steinkuhler, C.; Di Marco, S. *Proc. Natl. Acad. Sci. U.S.A.* **2004**, *101*, 15064.
17. Witter, D. J.; Belvedere, S.; Chen, L.; Secrist, J. P.; Mosley, R. T.; Miller, T. A. *Bioorg. Med. Chem. Lett.* **2007**, *17*, 4562.